Journal of Thermal Analysis and Calorimetry, Vol. 85 (2006) 3, 795–800

PREPARATION AND THERMAL DECOMPOSITION STUDY OF PYRIDINEDICARBOXYLATE INTERCALATED LAYERED DOUBLE HYDROXIDES

*M. Wei**, *X. Y. Xu, J. He, G. Y. Rao and H. L. Yang*

State Key Laboratory of Chemical Resource Engineering, Beijing University of Chemical Technology, Beijing 100029, P.R. China

Supramolecular 2,3- and 2,5-pyridinedicarboxylate (PDC) intercalated ZnAl-layered double hydroxides (2,3- and 2,5-PDC–ZnAl–LDHs) have been prepared by ion exchange method. The structure and composition of the intercalated materials have been studied by X-ray diffraction (XRD) and inductively coupled plasma emission spectroscopy (ICP). The study indicates that the 2,3-PDC and 2,5-PDC anions are accommodated as interdigitated bilayer and monolayer arrangement respectively between the sheets of LDHs. Furthermore, their thermal decomposition processes were studied by the use of in situ high temperature X-ray diffraction (HT-XRD), and the combined technique of thermogravimetry-differential thermal analysis-mass spectrometry (TG-DTA-MS) under N_2 atmosphere. Based on the comparison study on the temperatures of both decarboxylation and complete decomposition of interlayer PDC, it can be concluded that 2,5-PDC–ZnAl–LDHs has higher thermal stability than that of 2,3-PDC–ZnAl–LDHs.

Keywords: *intercalation, layered double hydroxides, pyridinedicarboxylate, thermal decomposition*

Introduction

Layered double hydroxides (LDHs) belong to the clay family. The general formula for these compounds can be represented as $[M^{II}_{1-x}\ M^{III}_{x}(OH)_2]^{x+}(A^{n-})_{x/n}\cdot mH_2O$, where M^{II} and M^{III} are di- and trivalent metals, such as Zn^{2+}, Ni^{2+}, Mg^{2+}, Al^{3+} and Fe^{3+}, respectively, and A is an anion. The main component of the LDHs is composed of infinite sheets of positively charged brucite-type $Mg(OH)_2$, where trivalent cations have replaced a fraction x of the divalent cations in octahedral coordination. LDHs have attracted interest due to their ability to exchange their anions for other negatively charged species [1–11]. The replacement of inorganic anions with organic species yields modified organo-LDHs, which have potential application such as nanocomposites [12, 13], drug delivery reagents [14, 15], catalysts [16–18] and adsorbents [19].

Recently, anionic drug molecules have been intercalated into a variety of LDHs [20, 21], with aim to determine the feasibility of using these intercalation compounds as materials for the storage, transport and ultimately controlled release of the drug. 2,3- and 2,5-PDC are drug intermediates which have potent biological activity, and there are very few reports about PDC intercalated into LDHs. In this paper we report the preparation and characterization of 2,3- and 2,5-PDC intercalated ZnAl–LDHs. Furthermore, a combination of technique including in situ HT-XRD and TG-DTA-MS has been used to investigate the thermal decomposition process of the composites. Therefore, this work provides an understanding of the thermal stability of drug-LDH hybrid for prospective application as the basis of a novel drug delivery system.

Experimental

Sample preparation

The precursor ZnAl–NO_3–LDHs was synthesized by coprecipitation. Typically, an aqueous solution of NaOH (0.6 mol) in 40 mL deionized water was added dropwise to a vigorously stirred freshly prepared solution containing $Zn(NO_3)_2\cdot 6H_2O$ (0.2 mol) and $Al(NO_3)_3\cdot 9H_2O$ (0.1 mol) (Zn^{2+}/Al^{3+}=2) in 100 mL deionized water under a nitrogen atmosphere at 70°C. The final pH was ca. 8. The resulting slurry was aged with stirring at 70°C for 48 h. The solid precipitate was collected by filtration using a membrane filter under suction, washed thoroughly with water and dried at 70°C for 18 h.

The intercalation compounds of both 2,3- and 2,5-PDC–ZnAl–LDHs were synthesized by ion exchange method. A solution of 2,3- or 2,5-PDC (1.8 g, 0.011 mol) in 50 mL deionized water was added to a suspension of ZnAl–NO_3–LDHs (1.5 g, ca. 0.012 mol) in 50 mL water, and the solution pH was kept 5.0 by adding 0.1 mol L^{-1} NaOH solution during reaction. The mixture was heated at 70°C under a nitrogen atmosphere for 24 h. The product was washed extensively with deionized water, centrifuged and dried at 70°C for 18 h.

* Author for correspondence: weimin@mail.buct.edu.cn

1388–6150/$20.00

Akadémiai Kiadó, Budapest, Hungary
Springer, Dordrecht, The Netherlands

Experimental techniques

In situ XRD patterns were performed on a Shimadzu XRD-6000 diffractometer in the temperature range 25–600°C under N_2 atmosphere, using CuK_α radiation (γ=1.542 Å) at 40 kV, 30 mA. The samples as unoriented powders were scanned in steps of 0.02° in the 2θ range 3–70° using a count time of 4 s per step. Infrared spectra of samples were recorded using a Brucker Vector 22 model Fourier transform infrared spectrometer (FTIR). Specimens were tested in the form of KBr pellet.

TG-DTA analysis were performed on a Seiko 6300 simultaneous DTA-TGA from Seiko Instruments with a heating rate of 10°C min^{-1} under N_2 atmosphere (flux of 100 cm^3 min^{-1}) in the temperature range 25–600°C. Simultaneous TG-MS analysis was performed in a Pyris Diamond TG-DTA coupled to ThermoStar^{TM} QM220 mass spectrometer by a quartz capillary transfer line. Elemental analysis of the metal contents was performed on an ICPS-7500 model inductively coupled plasma emission spectroscopy. C, H and N elemental analysis were carried out with an elementar vario model elemental analyzer.

Results and discussion

The crystalline structure and chemical composition of 2,3- and 2,5-PDC–ZnAl–LDHs

Figure 1 shows the XRD patterns of ZnAl–NO_3–LDHs, 2,3- and 2,5-PDC–ZnAl–LDHs, and the corresponding indexing parameters are listed in Table 1. It can be seen that all of the samples show an XRD pattern characteristic of LDH-like materials. Compared with ZnAl–NO_3–LDHs (d_{003}=0.893 nm), both 2,3- and 2,5-PDC–ZnAl–LDHs exhibit a significant expansion of the interlayer domain (d_{003}=1.561 and 1.382 nm respectively), which is indicative of successful intercalation.

Figure 2 displays the FTIR spectra of the three samples. The absorption band at around 3423 cm^{-1} in the FTIR spectrum for 2,5-PDC–ZnAl–LDHs (Fig. 2c) is attributed to OH stretching arising from the hydroxyl groups of LDHs and/or physically adsorbed water molecules. The characteristic bands at 1609 and 1395 cm^{-1} are assigned to the asymmetric and symmetric stretching vibration of carboxylate group of 2,5-PDC anions, indicating a successful intercalation. The weak shoulder at around 1365 cm^{-1} indicates the presence of little contamination of carbonate. In the case of 2,3-PDC–ZnAl–LDHs (Fig. 2b), a broad peak centered at about 3448 cm^{-1} is attributed to OH stretching. It can be seen that there was some difference in the absorption bands of carboxylate group compared with those of 2,5-PDC–ZnAl–LDHs. The asymmetric stretching

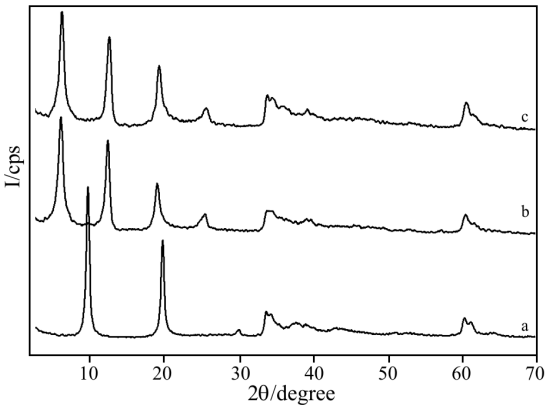

Fig. 1 XRD patterns of a – ZnAl–NO_3–LDHs, b – 2,3-PDC–ZnAl–LDHs and c – 2,5-PDC–ZnAl–LDHs

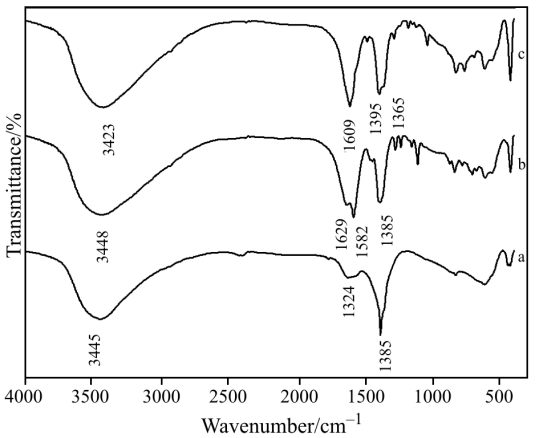

Fig. 2 FTIR spectra of a – ZnAl–NO_3–LDHs, b – 2,3-PDC–ZnAl–LDHs and c – 2,5-PDC–ZnAl–LDHs

Table 1 XRD parameters of ZnAl–NO_3–LDHs, 2,3- and 2,5-PDC–ZnAl–LDHs

Parameter	ZnAl–NO_3–LDHs	2,3-PDC–ZnAl–LDHs	2,5-PDC–ZnAl–LDHs
d_{003}/nm	0.893	1.561	1.382
d_{110}/nm	0.153	0.153	0.152
Gallery height/nm	0.413	1.081	0.902
*Length of acid anion/nm	0.249	0.592	0.768
Lattice parameter *c*/nm	2.679	4.638	4.146
Lattice parameter *a*/nm	0.306	0.306	0.304

*calculated by ChemWin 6.0

Table 2 Chemical composition of 2,3- and 2,5-PDC–ZnAl–LDHs

Samples	Element	Calc. mass%	Exp. mass%	Chemical composition
2,3-PDC–ZnAl–LDHs	Zn	32.39	32.28	$[Zn_{0.649}Al_{0.351}(OH)_2]\ (NO_3^-)_{0.029}$ $(C_7H_3NO_4^{2-})_{0.161}\cdot 0.9H_2O$
	Al	7.28	7.31	
	C	10.39	10.27	
	H	3.29	3.21	
	N	2.04	2.03	
2,5-PDC–ZnAl–LDHs	Zn	33.91	33.81	$[Zn_{0.653}Al_{0.347}(OH)_2]\ (NO_3^-)_{0.017}$ $(CO_3^{2-})_{0.013}(C_7H_3NO_4^{2-})_{0.151}\cdot 0.7H_2O$
	Al	7.49	7.50	
	C	10.26	10.11	
	H	3.08	3.03	
	N	1.34	1.45	

vibration of carboxylate group was demonstrated to be the overlapped two-peak band at 1629 and 1582 cm^{-1} respectively, which is much different from the FTIR spectra of other reports on intercalated organic carboxylate in which only one-peak band can be observed for the asymmetric stretching vibration of carboxylate group [22, 23]. The broad band at 1385 cm^{-1} is due to both the symmetric stretching vibration of carboxylate of 2,3-PDC and the stretching vibration of nitrate. The double peak of asymmetric stretching vibration of carboxylate group may indicate that there were two different host-guest interactions between the host layer and the two adjacent carboxyl groups of interlayer 2,3-PDC anions, which will be further confirmed by TG-MS.

Based on elemental analysis, the chemical composition of 2,3- and 2,5-PDC–ZnAl–LDHs (Zn/Al=2) are listed in Table 2. It can be seen that NO_3^- was co-intercalated into both of the two composites, and some little contamination of carbonate was also found in 2,5-PDC–ZnAl–LDHs, which is in accordance with the results of FTIR.

Study on thermal decomposition process

The XRD parameters of 2,3- and 2,5-PDC–ZnAl–LDHs show that the interlayer distance are 1.561 and 1.382 nm, respectively. Taking into account the layer thickness of brucite (0.48 nm), the gallery height was calculated to be 1.081 and 0.902 nm, respectively. Comparison of the length of 2,3-PDC (0.592 nm) with a gallery height of 1.081 nm suggests that the anions are accommodated as an interdigitated bilayer arrangement with the two adjacent carboxyls of individual anion attaching simultaneously to the upper or lower hydroxide layers. Moreover, the existence of hydrogen bonding interactions between hydroxyl groups and interlayer water molecules may lead to the stability of this composite structure. A schematic representation of the probable arrangement for 2,3-PDC–ZnAl–LDHs is shown in Fig. 3a. While in the case of 2,5-PDC–ZnAl–LDHs, the length of anion (0.768 nm) indicates that the guest are accommodated as a monolayer of species with their opposite carboxyls of individual anion attaching respectively to the upper and lower hydroxide lamella, as shown in Fig. 3b.

The TG-MS profiles of 2,3-PDC–ZnAl–LDHs under N_2 atmosphere are displayed in Fig. 4. It exhibits four mass loss events according to the DTG curve. The first event in the temperature range 25–197°C is attributed to the loss of the surface adsorbed and interlayer water, corresponding to the *m*/*z* 18 peak observed at about 171°C. The second event from 197 to 271°C is due to dehydroxylation of the LDHs layers and partial decarboxylation of the interlayer 2,3-PDC. The second *m*/*z* 18 peak at about 289°C is attributed to dehydroxylation of the LDHs layers, and the *m*/*z* 44 signal (due to CO_2) occurred at about 238°C results from the decarboxylation of 2,3-PDC. The third event (271–344°C) is related to dehydroxylation of the LDHs layers, loss of the interlayer nitrate and decarboxylation of the interlayer 2,3-PDC. The weak

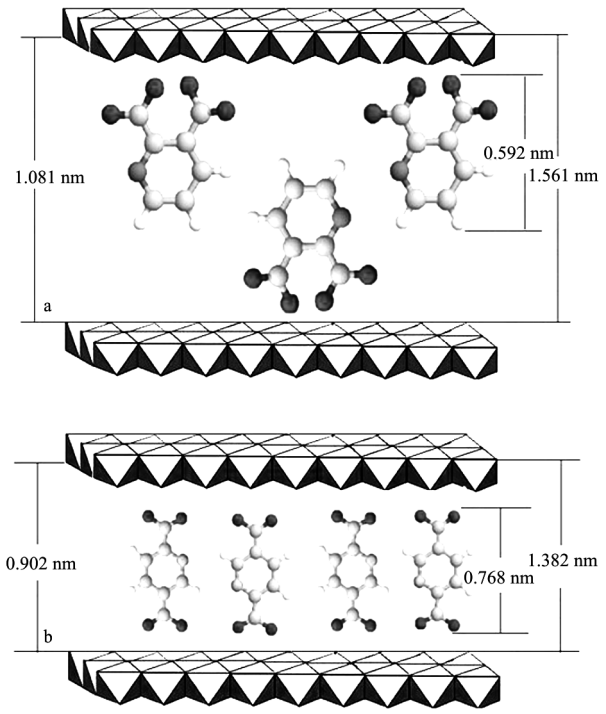

Fig. 3 Schematic representation of the possible arrangements for a – 2,3-PDC–ZnAl–LDHs and b – 2,5-PDC–ZnAl–LDHs

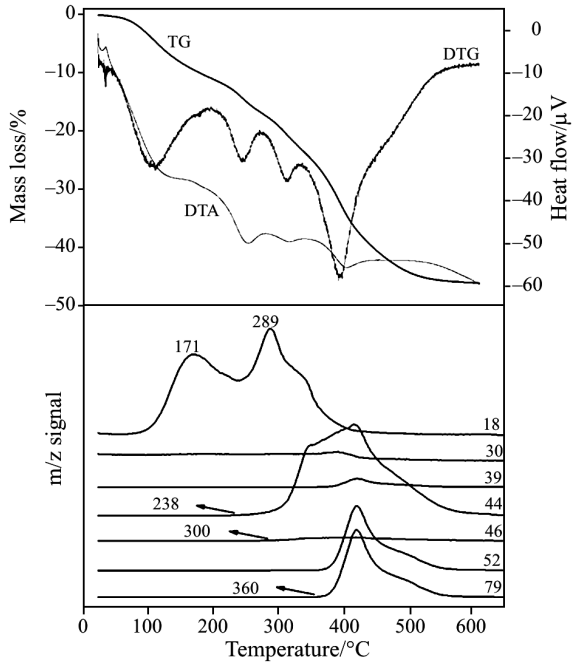

Fig. 4 TG-MS profiles of 2,3-PDC–ZnAl–LDHs under N_2 atmosphere. The *m*/*z* peaks correspond to the following fragments: H_2O (18), NO (30), C_2HN (39), CO_2 (44), NO_2 (46), C_4H_4 (52) and pyridine (79)

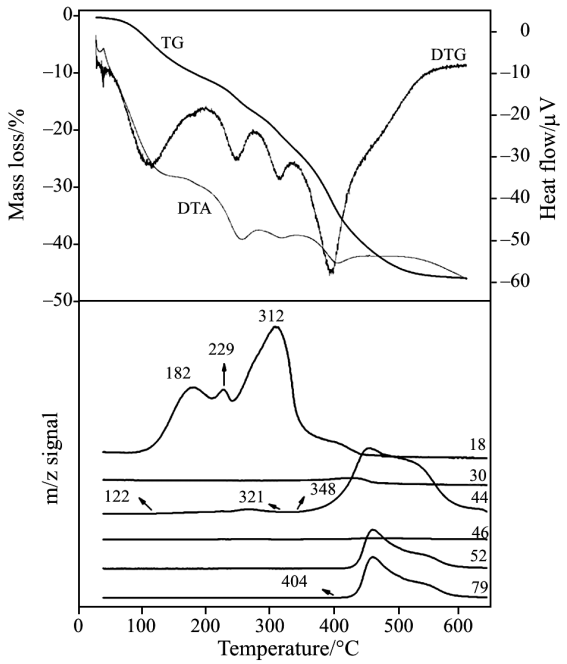

Fig. 5 TG-MS profiles of 2,5-PDC–ZnAl–LDHs under N_2 atmosphere. The *m*/*z* peaks correspond to the following fragments: H_2O (18), NO (30), CO_2 (44), NO_2 (46), C_4H_4 (52) and pyridine (79)

m/*z* 30 signal (due to NO) and the *m*/*z* 46 signal (due to NO_2) occurred at approximately 300°C correspond to the decomposition of a small amount of impurity nitrate. The last mass loss between 344 and 600°C is the result of further dehydroxylation of the LDHs layers and the complete decomposition of the interlayer guest. The *m*/*z* 79 signal (due to pyridine), the *m*/*z* 52 signal (due to C_4H_4) and the *m*/*z* 39 signal (due to C_2HN) occurred at approximately 360°C correspond to the complete decomposition of 2,3-PDC anions. It can be observed that the decomposition of 2,3-PDC ring occurred at approximately 360°C, which is much higher than that of decarboxylation of the interlayer 2,3-PDC (238°C). This is an indication that the decomposition of the interlayer 2,3-PDC includes two stages: first is the partial decarboxylation of the 2,3-PDC anions, and the second stage is the complete decomposition. The results by TG-MS is in accordance with those of FTIR to some extent in which one two-peak band was observed for the asymmetric vibrational absorption of carboxyl and thus two different host-guest interactions existed between the layers. The carboxyl which interacts with the host layers weakly might decompose firstly, and then another carboxyl as well as the decomposition of PDC ring.

The TG–MS profiles of 2,5-PDC–ZnAl–LDHs under N_2 atmosphere are shown in Fig. 5. The thermal decomposition of 2,5-PDC–ZnAl–LDHs was similar to that of 2,3-PDC–ZnAl–LDHs. Three *m*/*z* 18 peaks were observed: the first at about 182°C and the second at 229°C are attributed to the loss of the surface adsorbed and interlayer water and the third at about 312°C is associated with dehydroxylation of the LDHs layers. The weak *m*/*z* 46 signal (due to NO_2) and the small *m*/*z* 30 signal (due to NO) occurred at approximately 309°C correspond to the decomposition of interlayer nitrate. Two *m*/*z* 44 (due to CO_2) peaks were observed. The first weak one, in the temperature range 122–321°C results from the decomposition of a small amount of impurity carbonate anions, which has not been found in 2,3-PDC–ZnAl–LDHs. This is in agreement with the results of elemental analysis (Table 2). The second rather strong *m*/*z* 44 signal occurred at about 348°C is attributed to the decarboxylation of 2,5-PDC. The *m*/*z* 79 signal (due to pyridine) and the *m*/*z* 52 signal (due to C_4H_4) occurred at approximately 404°C correspond to the complete decomposition of 2,5-PDC anions. Compared with 2,3-PDC–ZnAl–LDHs, it can be seen that the temperature of decarboxylation of the interlayer 2,5-PDC (348°C) is much higher than that of 2,3-PDC–ZnAl–LDHs (238°C), indicating that the host-guest interaction in 2,5-PDC–ZnAl–LDHs is stronger than that of in 2,3-PDC–ZnAl–LDHs. It also can be seen that the temperature of the complete decomposition of 2,5-PDC (404°C) is higher than that of 2,3-PDC–ZnAl–LDHs (360°C), which further confirms the conclusion that the former composite has higher thermal stability than the latter.

The in situ HT-XRD patterns of 2,3-PDC–ZnAl–LDHs in the temperature range

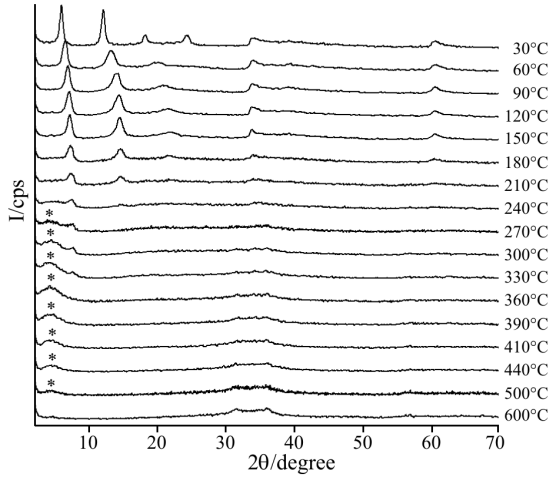

Fig. 6 In situ HT-XRD patterns of 2,3-PDC–ZnAl–LDHs in the temperature range 30–600°C under N_2 atmosphere

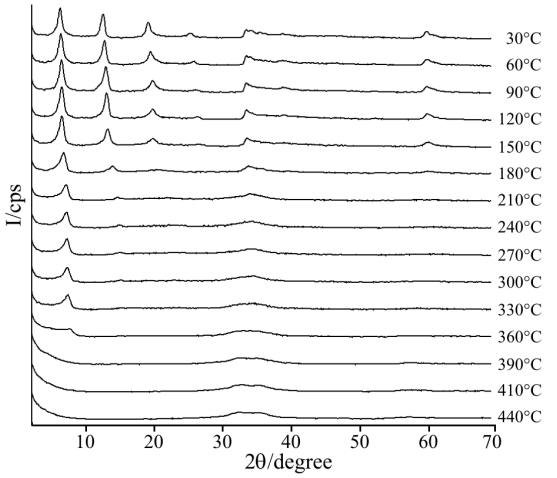

Fig. 7 In situ HT-XRD patterns of 2,5-PDC–ZnAl–LDHs in the temperature range 30–440°C under N_2 atmosphere

30–600°C under N_2 atmosphere are displayed in Fig. 6. It can be observed in Fig. 6 that the (003), (006) and (009) reflections of 2,3-PDC–ZnAl–LDHs clearly moved to higher-angle 2θ with the increase of temperature. There was a decrease in d_{003} basal spacing from 1.561 (30°C) to 1.218 nm (180°C). Since there was no decomposition of 2,3-PDC in this temperature range confirmed by TG-MS (Fig. 4), the decrease in d_{003} is possibly related to two reasons: (1) the destruction of hydrogen bonding area as a result of deintercalation of interlayer water molecules, which has been demonstrated by other researchers [24]; (2) the re-orientation of the interlayer guest anions. When the temperature was above 210°C, the (006) and (009) reflections of 2,3-PDC–ZnAl–LDHs disappeared, indicating that there was a major structural change resulting from decrease in sequence order. The further decrease in d_{003} value from 210 to 330°C is attributed to the decomposition of interlayer guest anions, which is in consistence with the results by TG-MS (Fig. 4) that the decomposition occurred at about 238°C. The (003) reflection of 2,3-PDC–ZnAl–LDHs disappeared at 360°C, implying the complete collapse of the layered structure. It can be seen that a new peak was observed at about 270°C (marked with * in Fig. 6) and disappeared at about 500°C, which indicates that a new phase formed in this range, however, its definite structure was unknown.

The in situ HT-XRD patterns of 2,5-PDC–ZnAl–LDHs in the temperature range 30–440°C under N_2 atmosphere are shown in Fig. 7. Compared with the in situ HT-XRD patterns of 2,3-PDC–ZnAl–LDHs, there are mainly two differences. Firstly, it can be observed in Fig. 7 that there was a decrease in d_{003} basal spacing from 1.382 (30°C) to 1.320 nm (180°C). The value of decrease in d_{003} is 0.062 nm, which is smaller than that of 2,3-PDC–ZnAl–LDHs (0.343 nm). This indicates the

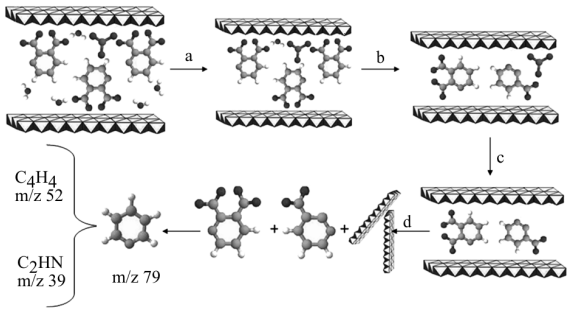

Fig. 8 A schematic representation of thermal decomposition process of 2,3-PDC–ZnAl–LDHs; a – loss of water, b – dehydroxylation of the LDHs layers and partial decarboxylation, c – decomposition of nitrate and decarboxylation of the interlayer 2,3-PDC, d – complete decomposition

lower water content in 2,5-PDC–ZnAl–LDHs (actually been confirmed by TG curve in mass loss in 30–180°C) and thus thinner hydrogen bonding area which might lead to stronger host-guest interaction, compared with 2,3-PDC–ZnAl–LDHs. As a result, the thermal stability of 2,5-PDC–ZnAl–LDHs is higher than that of 2,3-PDC–ZnAl–LDHs. Secondly, the complete collapse of the layered structure of 2,5-PDC–ZnAl–LDHs occurred at 390°C (at which the (003) reflection disappeared, as shown in Fig. 7), which is higher than that of 2,3-PDC–ZnAl–LDHs (360°C, Fig. 6), further indicating the higher thermal stability of 2,5-PDC–ZnAl–LDHs.

Conclusions

In this paper, 2,3- and 2,5-PDC intercalated LDHs composites have been synthesized by the method of ion exchange. Based on XRD, IR, and elemental analysis of the resulting intercalates, schematic representation of the possible arrangements for interlayer an-

ions have been proposed. The study indicates that the 2,3-PDC anions are accommodated as an interdigitated bilayer arrangement with the two adjacent carboxyls of individual anion attaching simultaneously to the upper or lower hydroxide layers, while 2,5-PDC anions are accommodated as a monolayer of species with their opposite carboxyls of individual anion attaching respectively to the upper and lower hydroxide lamella. Furthermore, TG-DTA-MS and in situ HT-XRD were used to investigate their thermal decomposition process under N_2 atmosphere in detail.

Both of the two samples exhibit four main decomposition events as shown in Fig. 8 (2,3-PDC–ZnAl–LDHs was selected as an example). The first event is attributed to the loss of the surface adsorbed and interlayer water, corresponding to the decrease in d_{003} basal spacing with the increase of temperature. The second event is due to dehydroxylation of the LDHs layers and partial decarboxylation of the interlayer PDC anions, accompanied with the decrease in d_{003} and the disappearance of the (006) and (009) reflections resulting from decrease in sequence order. The third event is related to dehydroxylation of the LDHs layers, decomposition of the little contamination nitrate/carbonate and decarboxylation of the interlayer 2,3-PDC. The last event is related to further dehydroxylation of the LDHs, complete decomposition of PDC which leads to collapse of the layered structure.

Based on the comparison study on the temperatures of both decarboxylation and complete decomposition of interlayer PDC, it can be concluded that 2,5-PDC–ZnAl–LDHs has higher thermal stability than that of 2,3-PDC–ZnAl–LDHs.

Acknowledgements

This project was supported by the National Natural Science Foundation Key Project of China (Project No.: 90306012), the National Basic Research Program (973 Program) (Project No.: 2004CB720602), the Beijing Nova Program (No.: 2004A13), and the Program for Changjiang Scholars and Innovative Research Team in University (PCSIRT).

References

1 F. Cavani, F. Trifiro and A. Vaccari, Catal. Today, 11 (1991) 173.
2 P. Bharali, R. Saikia, R. K. Boruah and R. L. Goswamee, J. Therm. Anal. Cal., 78 (2004) 831.
3 J. H. Choy, S. Y. Kwak, Y. J. Jeong and J. S. Park, Angew. Chem. Int. Ed., 22 (2000) 4042.
4 P. Kustrowski, A. Wegrzyn, L. Chmielarz, A. Bronkowska, A. Rafalska-Iasocha and R. Dziembaj, J. Therm. Anal. Cal., 77 (2004) 243.
5 J. H. Choy, S. M. Paek, J. M. Oh and E. S. Jang, Current Appl. Phys., 2 (2002) 489.
6 T. W. Nicola, J. V. Paula and M. Stephen, J. Mater. Chem., 7 (1997) 1623.
7 A. Fudala, I. Palinko and I. Kiricsi, Inorg. Chem., 38 (1999) 4653.
8 S. P. Newman and W. Jones, New J. Chem., 22 (1998) 105.
9 F. Kovanda, V. Balek, V. Dorničák, P. Martinec, M. Mašláò, L. Bílková, D. Koloušek and I. M. Bountsewa, J. Therm. Anal. Cal., 71 (2003) 727.
10 B. Lotsch, F. Millange, R. I. Walton and D. O'Hare, Solid State Sciences, 3 (2001) 883.
11 A. Beres, I. Palinko, A. Fudala, I. Kiricsi, Y. Kiyozumi, F. Mizukami and J. B. Nagy, J. Therm. Anal. Cal., 56 (1999) 311.
12 M. D. Arco, D. Carriazo, S. Gutierrez, C. Martin and V. Rives, Inorg. Chem., 43 (2004) 375.
13 O. C. Wilson, T. Olorunyolemi, A. Jaworski and L. Borum, Appl. Clay Sci., 15 (1999) 265.
14 V. Ambrogi, G. Fardella, G. Grandolini and L. Perioli, Int. J. Pharm., 220 (2001) 23.
15 A. I. Khan, L. Lei, A. J. Norquist and D. O'Hare, Chem. Commun., (2001) 2342.
16 M. C. Boyapati, S. C. Naidu, J. Karangula and L. K. Mannepalli, J. Am. Chem. Soc., 124 (2002) 5341.
17 W. Kagunya, Z. Hassan and W. Jones, Inorg. Chem., 35 (1996) 5970.
18 B. M. Choudary, M. L. Kantam, B. Kavita, C. V. Reddy and F. Figueras, Tetrahedron, 56 (2000) 9357.
19 G. N. Manju, M. C. Gigi and T. S. Anirudhan, Int. J. Chem. Technol., 6 (1999) 134.
20 M. Wei, S. X. Shi, J. Wang, Y. Li and X. Duan, J. Solid State Chem., 177 (2004) 2534.
21 B. X. Li, J. He, D. G. Evans and X. Duan, Int. J. Pharm., 287 (2004) 89.
22 C. Vaysse, L. Guerlou-Demourgues, E. Duguet and C. Delmas, Inorg. Chem., 42 (2003) 4559.
23 M. Borja and P. K. Dutta, J. Phys. Chem., 96 (1992) 5434.
24 V. Prevot, C. Forano and J. P. Besse, Inorg. Chem., 37 (1998) 4293.

Received: December 5, 2005
Accepted: March 21, 2006
OnlineFirst: July 20, 2006

DOI: 10.1007/s10973-005-7468-z